



iJRASET

International Journal For Research in
Applied Science and Engineering Technology



INTERNATIONAL JOURNAL FOR RESEARCH

IN APPLIED SCIENCE & ENGINEERING TECHNOLOGY

Volume: 9 Issue: VI Month of publication: June 2021

DOI: <https://doi.org/10.22214/ijraset.2021.35163>

www.ijraset.com

Call:  08813907089

E-mail ID: ijraset@gmail.com

Multi-Core Surface Plasmon Resonance Refractive Index Sensor on Photonic Crystal Fiber

Harshit Bhargava¹, Partha Saha²

¹Electronics and Communicatio, Harcourt Butler Technical University

²Assistant Professor, Electronics and Communication, Harcourt Butler Technical University

Abstract: In this research work, low refractive index (RI) detection done on multi-core photonic crystal fiber (PCF) based highly sensitive surface plasmon resonance (SPR) sensor is propounded. Sensing the changes in neighboring medium's refractive index is done by placing the plasmonic material i.e. Silver (Ag) over the crystal structure of fiber. On top of the Silver, a threadlike film of titanium dioxide (TiO₂) is deposited to prevent oxidation of plasmonic material silver. Peak wavelength sensitivity thus achieved by this sensor is 127,600 nm/RIU and similarly, peak amplitude sensitivity achieved is 2561 RIU⁻¹, respectively. Subsequently making this sensor suitable candidate for various applications such as biosensing, sensing organic compounds and chemicals, inspecting pharmaceuticals and other detections.

Index Terms: Refractive Index, Surface Plasmon Resonance, Photonic crystal fiber, Sensor.

I. INTRODUCTION

An optical phenomenon which occurs due to oscillation of free electrons at the interfacing of dielectric material and metallic surface is known as Surface Plasmon Resonance. Due to this process, SPR sensors are being broadly premeditated because of provided nice features such as ability to choose and meticulousness in detection, quick action, actual- time and effective light-manipulating abilities. The orthodox SPR sensors are designed which base on the prism, slot waveguide, fiber Bragg grating and V-groove waveguide which make the system large and expensive. To overcome these limitations, Surface Plasmon Resonance sensors constructed on PCF are being planned that confirms mobility, optimized structure and capability to detect from distances. Variety of photonic crystal fibers are worked with several arrangements for sensing based on surface plasmon resonance submissions such as microfluidic structures based on slot using structures, D-shaped structures, layered by metal internally, and many more.

Surface Plasmon Resonance sensor based on Photonic Crystal Fiber encompasses two types of detecting plans: internally & externally. The air holes are purposefully fill the analyte in internal detection. This detecting method displays greater sensitivity as surrounded analyte openly fluctuates the original distribution of fiber's refractive index. Although, Feasibility gets invalid internal method of detection for the instantaneous and dispersed detection solicitation. Additionally, this method is incredibly laborious to implement and also involvements larger transmission deficit. Downsides of detecting internally could be overwhelmed via introducing the liquid of which detection is to be performed on at the outer surface of the PCF, who is accredited as external detection method. At present, this method became widely known because of its meek recognition and hands-on operation tactic.

Several other PCF based Surface Plasmon Resonance sensors which are proficient in recognizing the index of refraction of congener with range beginning from 1.33 are described at many of the related recent research works. Majority of the research studies highlight the detection layout recognize substance to have refractive index greater than 1.43. Not many studies are ever been done at Photonic Crystal Fiber Surface Plasmon Resonance devices which are able to find lesser refractive index a smaller amount than 1.43. Recently, plenty of submissions are emerging in which small refractive index are needed to be recognized, for-example pharmaceutical medicines, halide-containing organic compounds, aerogel, and many others. Bearing in mind, the truth that there are Photonic Crystal Fiber Surface Plasmon Resonance sensors emerging in the modern-day scenario that are fit for sensing lesser Refractive Index of substance smaller to 1.40. Greatest Wavelength Sensitivity by the devices calculated so far lie in the range of 6000-51,000 nm/RIU. However, Amplitude Sensitivity has been calculated not in many studies and the ones calculated are in the range of about 1000-2000 RIU⁻¹. This designates sufficient possibility that Photonic Crystal Fiber based Surface Plasmon Resonance sensor can detect smaller values of refractive index and with improved detectivity at both examining plans.

In this paper, Photonic Crystal fiber based Surface Plasmon resonance Sensor is successfully structured and arithmetically studied to detect the lower refractive index. Multiple sensing channel & configuration between two different metals accentuates sensitivity in wavelength and amplitude examination approaches. TiO₂ positioned above the plasmonic material harvests great amount of charge carriers from the interface and field from the core incorporates with plasmonic part. Analytical outcomes show peak values in spectral sensitivity of 127,600 nm/RIU and in amplitude sensitivity 2561 RIU⁻¹.

II. MATHEMATICAL PROPOSAL AND DEMONSTRATING

Cross-sectional view of specified device is portrayed in Fig. 1. The structure consists of silica as the material through which the light of a certain wavelength flows through and air holes acting as insulator preventing light to flow out of the fiber and be lost in nothingness. The silica structure is then surrounded by sheets of silver that run through the whole fiber which is playing the role of sensing the low refractive index. A threadlike layer of TiO_2 is placed above silver sheets to protect silver from oxidation from analyte and other stuff. Analyte is the material whose refractive index is being sensed here. PML is the layer of silica which prevents light from interacting with the fiber back after being lost by the fiber structure as it would affect the actual work of the sensor. Fig. 2 shows the probable creation method of the specified sensor. Primarily, altogether the supporting tubes and shafts are collected and formerly stretched at a specific speed recognized as the stack and stretch method to form fibers. Thin and thick hair rods and strong rods are used to make large, small and no ventilation holes respectively. After the fiber is manufactured, the polishing technology will be made workable. By the polishing process, part of the fiber as well as the large thin-walled capillary of the second ring will be polished. Then the chemical deposition method is made practical to coat silver and TiO_2 on the polished face of the fiber.

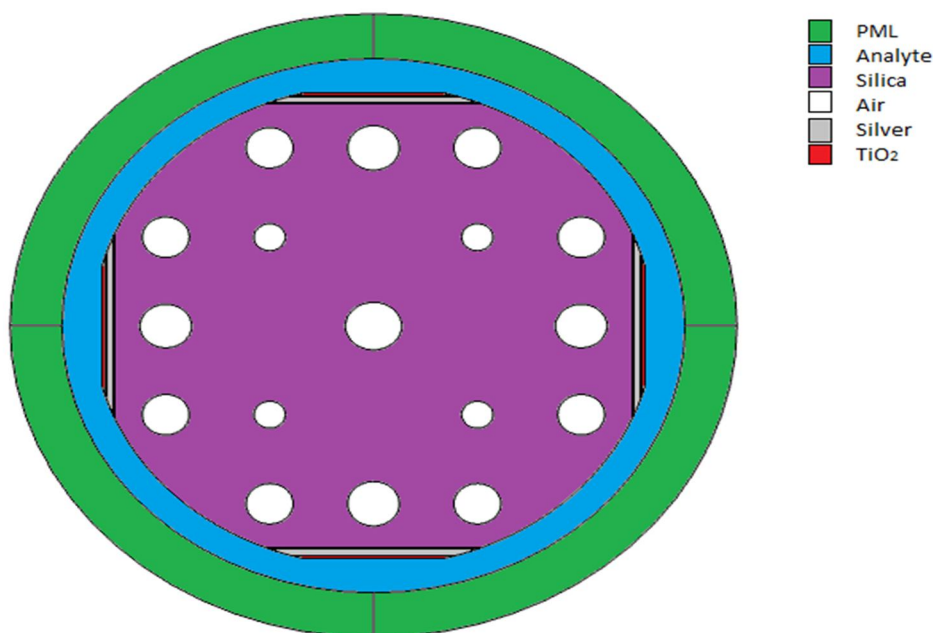


Fig. 1 Cross-sectional view

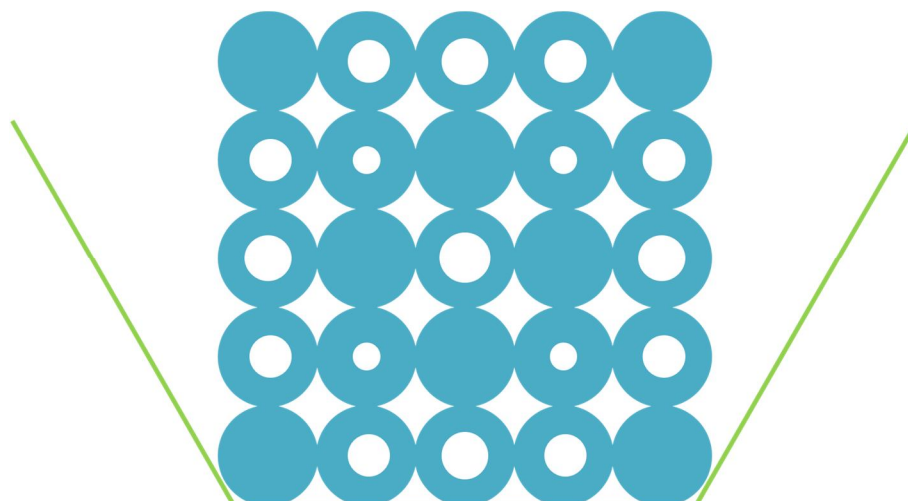


Fig. 2 Stacked preform process to manufacture fiber

COMSOL Multiphysics is the software used to perform simulations on proposed structure and do mathematical study. PML layer of silica is complemented as the outmost deposit to captivate radioactivity. Physics regulated normally fine mesh component is implemented to get simulation results. The diameters of the air holes takes is as follows: $d_1 = 1.80 \mu\text{m}$, $d_2 = 1.65 \mu\text{m}$, $d_3 = 1 \mu\text{m}$, $d_4 = 1.5 \mu\text{m}$. Lattice constant between two adjacent air holes is $A = 3.30 \mu\text{m}$, and thinness of the silver and TiO_2 are 55 nm and 10 nm, respectively. The ratio of electric permeability of silver to relative permeability of free space i.e. dielectric constant of the silver is attained using the Drude model. The backdrop stuff, SiO_2 is exercised of which RI is deliberated using the Sellmeier equation

$$n_{si}^2(\lambda) = 1 + \frac{B_1\lambda^2}{\lambda^2 - C_1^2} + \frac{B_2\lambda^2}{\lambda^2 - C_2^2} + \frac{B_3\lambda^2}{\lambda^2 - C_3^2} \quad (1)$$

where, Refractive Index of silica is denoted by n_{si} , the wavelength is represented by λ in μm and Sellmeier coefficients are denoted by B_1, B_2, B_3, C_1, C_2 and C_3 .

The dielectric constant of TiO_2 can be defined by the given equation.

$$n_{TiO_2}^2(\lambda) = 5.913 + \frac{2.441 \times 10^7}{\lambda^2 - 0.803 \times 10^7} \quad (2)$$

where, unit of λ is μm .

III. RESULTS

Fig. 3(a) shows the representation of field flowing through the fiber in center guided mode for the analyte with refractive index of 1.43. Fig. 3(b) represents the flow of field through the fiber in plasmonic mode. If there should arise an occurrence of center guided mode, the whole light field is encased at the center. Then again, the plasmonic mode is seen on the plasmonic material covered detecting medium. The field motion at the resonating point is presented in Fig. 3(c). Energy change technique between the core guided mode and the plasmonic mode due to strong coupling effect can moreover be seen from this figure. In Fig. 4, the dispersion accord of the initial mode and spectrum degradation is obtained. Indices of refraction of the SPP mode with order second and guiding mode of core meet at same point at λ_{op} of $1.72 \mu\text{m}$ for the analytics at RI of 1.36. It is supposed in this case the enthusiasm of the most of free electrons from the shoal is accountable for the larger fading field in the y-poles apart horizontal electric (TE) mode TEy contrast to TEx mode. When the phase complementing constrain is consummate, uttermost power shift can be attained from the basic guiding mode of core to the quantum dot mode. In the consequence, a crest is obtained at the point of junction.

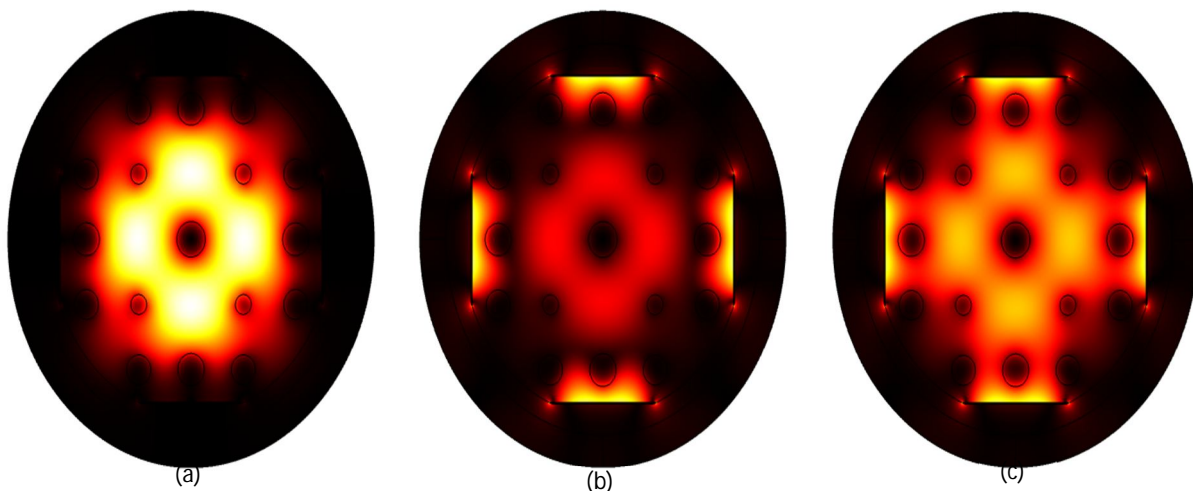


Fig. 3 Optical distribution of n_a 1.43 (a) core mode (b) plasmonic mode (c) resonance condition

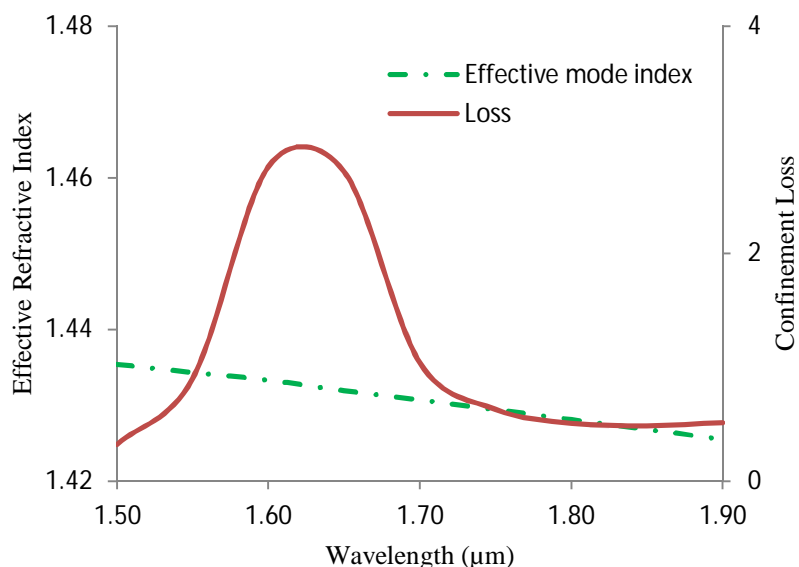


Fig. 4 Effective Refractive Index & Loss w.r.t. Wavelength

To estimate confinement loss of the device, subsequent equation has been used

$$\alpha = \frac{40 \pi \text{Im}(n_{eff})}{\ln(10) \lambda} \approx 8.686 \times k_0 \text{Imag}(n_{eff}) \times 10^4 \text{ dB/cm} \quad (3)$$

where, quantity of oscillations in allowed area is meant by, $k_0 = 2\pi/\lambda$, working frequency is signified by λ and unreal portion of the actual refractive index of the fiber is addressed by $\text{Imag}(n_{eff})$.

WS can be characterized by the condition 4. By applying condition 4, the proposed sensor shows most extreme Wavelength Sensitivity of 127,600 nm/RIU. At the point as the refractive index of analyte varies from 1.33 to 1.43 with a stage extent of 0.01, the projected device presents wavelength detectivity of 4500, 4500, 5500, 5500, 6500, 6500, 7500, 8500, 17000 and 127,600 nm/RIU, individually.

The smallest dispersion loss is discovered being 0.74 dB/cm at the functioning wavelength of 1340 nm while the most extreme misfortune is discovered to be 8.29 dB/cm at the reverberation frequency of 3110 nm. In addition at n_a 1.39, repression misfortune is discovered to be higher because of the solid coupling between center guided and SPP mode.

$$WS[nm/RIU] = \frac{\Delta\lambda_{peak}}{\Delta n_a} \quad (4)$$

Where $\Delta\lambda_{peak}$ specifies change in loss resonance peak & Δn_a denotes variation in refractive index of analyte.

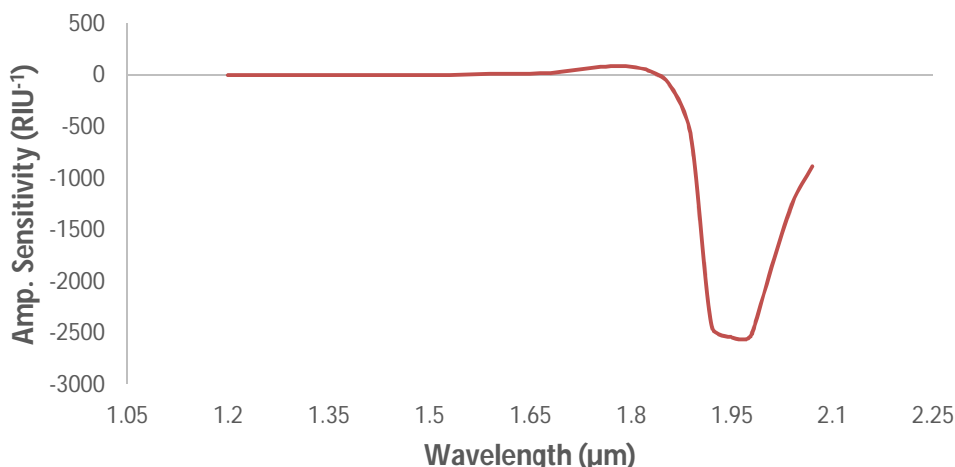


Fig. 5 Amplitude sensitivity with analyte RI 1.43

Amplitude Sensitivity of the projected device is premeditated by means of the succeeding Amplitude Sensitivity formulation, the projected device depicts the extreme Amplitude Sensitivity of 2561 RIU^{-1} for $n_a = 1.43$ and the minimum of 16 RIU^{-1} for $n_a = 1.13$. Fig. 5 shows Amplitude Sensitivity of the device for the discrepancies of analyte Refractive Index from 1.38 to 1.43 as an example.

$$AS[\text{RIU}^{-1}] = -\frac{1}{\alpha(\lambda, n_a)} \frac{\partial \alpha(\lambda, n_a)}{\partial n_a} \quad (6)$$

where, the confinement loss of the assumed analyte having Refractive Index n_a is shown as $\alpha(\lambda, n_a)$, the change amongst two loss ranges is represented by $\partial \alpha(\lambda, n_a)$ and variation in analyte Refractive Index is indicated by ∂n_a .

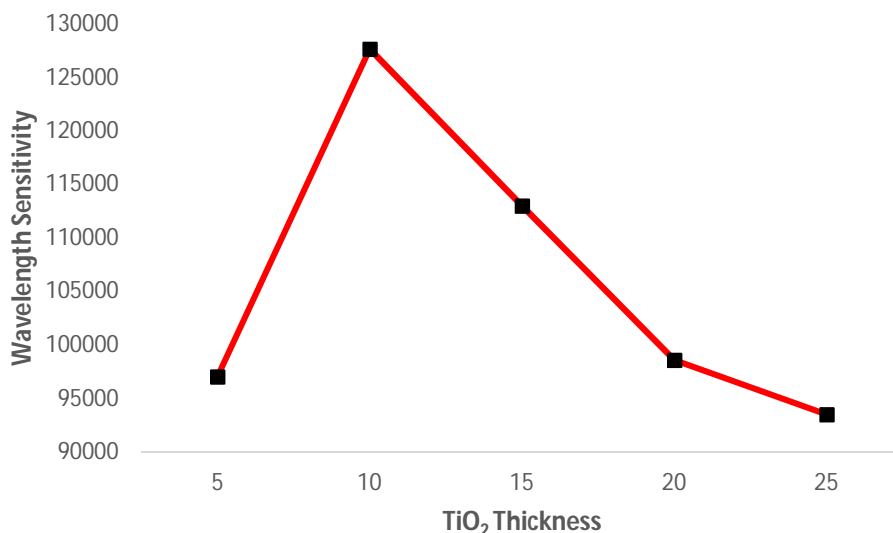


Fig. 6 Wavelength sensitivity for variation of TiO₂ Thickness

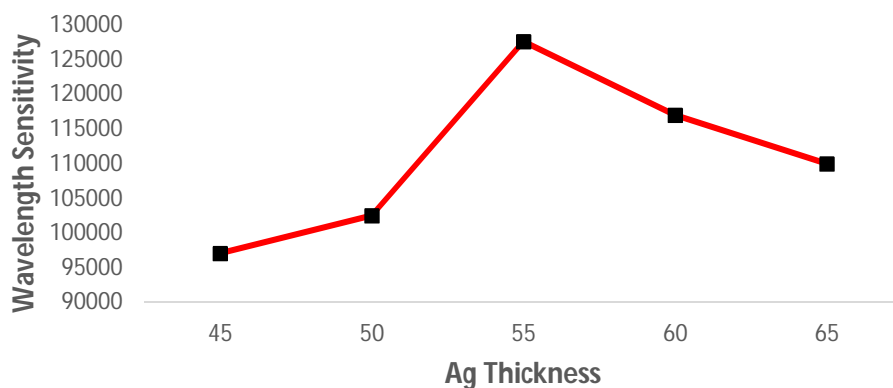


Fig. 7 Variation in Wavelength Sensitivity with varying Silver Thickness

Fig. 6 and 7 shows the way Wavelength Sensitivity changes with diverse values of silver and TiO₂ thickness respectively. It is observed that the maximum WS 127,600 nm/RIU is achieved at 55 nm Ag thickness and 10 nm TiO₂ thickness.

IV. CONCLUSIONS

A countless center intense plasmonic refraction record sensor for less refractive catalogue research work has been derived and mathematically observed. Several discovering mediums, such as Ag-TiO₂ design of the sensor became better the resounding effects combined carried out farthest sensitivities of 127,600 nm/RIU and 2561 RIU⁻¹ are provided usage of frequency and abundancy cross testing methods, individually, in the finding of scope of 1.29–1.39. Finally, exterior detecting devices and reasonable creation process made the derived sensor a solid opponent to acknowledge analytes with a less refractive record as checking and review in medical field, synthetics of bio-naturals, etc.

REFERENCES

- [1] R. C. Jorgenson and S. S. Yee, "A fiber-optic chemical sensor based on surface Plasmon resonance," *Sens. Actuators B* 12, 213–220(1993)
- [2] P. J. Kajenski, "Tunable optical filter using long-range surface Plasmons," *Opt. Eng.*, vol. 36, no. 5, pp. 1537–1541, May 1997
- [3] I. Stemmler, A. Brecht, and G. Gauglitz, "Compact surface Plasmon resonance-transducers with spectral readout for bio-sensing applications," *Sens. Actuator B, Chem.*, vol. 54, nos. 1–2, pp. 98–105, Jan. 1999
- [4] A. Khaleque and H. T. Hattori, "Ultra-broadband and compact polarization splitter based on gold filled dual-core photonic crystal fiber," *Journal of Applied Physics*, vol. 118, no. 14, p. 143101,
- [5] H. Reeves, J. Knight, P. S. J. Russell, and P. Roberts, "Demonstration of ultra-flattened dispersion in photonic crystal fibers," *Optics express*, vol. 10, no. 14, pp. 609–613, 2002
- [6] G. G. Nenninger, M. Piliarik and J. Homola, "Data analysis for optical sensors based on spectroscopy of surface Plasmon," *Meas. Sci. Technol.*, vol. 13, pp. 2038–2046 (2002)
- [7] C. Rhodes and S. Franzen, "Surface plasmon resonance in conducting metal oxides," *Journal Of Applied Physics*, vol. 100, pp.054905 (1-4) (2006)
- [8] I. M. White and X. Fan, "On the performance quantification of resonance refractive index sensors," *Optics Express*, vol. 16, no. 2, pp. 1020-1028(2008)
- [9] B. D. Gupta and R. K. Verma, "Surface plasmon resonance- based fiber optic sensors: principle, probe designs, and some applications," *Journal of sensors*, vol. 2009, pp. 1–12, 2009
- [10] X. Yu et al., "A selectively coated photonic crystal fiber based surface Plasmon resonance sensor," *J. Opt.*, vol. 12, pp. 015005-1–015005-4, (2010)
- [11] M. S. Luchansky, A. L. Washburn, T. A. Martin, M. Iqbal, L. C. Gunn, and R. C. Bailey, "Characterization of the field profile and bound mass sensitivity of a label-free silicon photonic microring resonator bio-sensing platform," *Biosensors and Bioelectronics*, vol.26, no. 4, pp. 1283–1291, 2010
- [12] F. Wang, Z. Sun, C. Liu, T. Sun, and P. K. Chu, "A highly sensitive dual-core photonic crystal fiber based on a surface Plasmon resonance biosensor with silver-grapheme layer," *Plasmonics*, 12, 1–7
- [13] B. Shuai, L. Xia, Y. Zhang, and D. Liu, "A multi-core holey fiber based plasmonic sensor with large detection range and high linearity," *Opt. Express* 20, 5974–5986 (2012)
- [14] The LHCb Collaboration, LHCb re-optimized detector design and performance E. K. Akowuah, T. Gorman, H. Ademgil, S. Haxha, G. K. Robinson, and J.V.Oliver, "Numerical analysis of a photonic crystal fiber for bio-sensing applications," *IEEE J. Quantum Electron* (2012)
- [15] Z. Tan · X. Li, Y. Chen and P. Fan, "Improving the sensitivity of fibersurface plasmon resonance sensor by filling liquid in a hollow core photonic crystal fiber," *Plasmonics*, vol. 9, no.1, pp 167–173 (2014)
- [16] Z. Fan, S. Li, Q. Liu, G. An, H. Chen, J. Li, D. Chao, H. Li, J. Zi, and W. Tian, "High sensitivity of refractive index sensor based on analyte filled photonic crystal fiber with surface Plasmon resonance," *IEEE Photon. J.* 7, 4800809 (2015)
- [17] A. A. Rifat, G. A. Mahdiraji, Y. M. Sua, Y. G. Shee, R. Ahmed, D. M. Chow, and F. R. M. Adikan, "Surface plasmon resonance photonic crystal fiber biosensor: a practical sensing approach," *IEEE Photon. Technol. Lett.* 27, 1628–1631 (2015)
- [18] P. Singh, "SPR biosensors: historical perspectives and current challenges," *Sens. Actuators B* 229, 110–130 (2016)
- [19] A. A. Rifat, G. A. Mahdiraji, Y. M. Sua, R. Ahmed, Y. G. Shee and F. R. M. Adikan, "Highly sensitive multi-core flat fiber surface plasmon resonance refractive index sensor," *Optics express*, vol.24, no. 3, pp. 2485–2495, 2016
- [20] Y. Chen, Q. Xie, X. Li, H. Zhou, X. Hong, and Y. Geng, "Experimental realization of D-shaped photonic crystal fiber SPR sensor," *J. Phys. D50*, 025101 (2017)
- [21] X. Yang, Y. Lu, B. Liu, and J. Yao, "Analysis of graphene-based photonic crystal fiber sensor using birefringence and surface plasmon resonance," *Plasmonics*, vol. 12, no. 2, pp. 489–496, 2017



10.22214/IJRASET



45.98



IMPACT FACTOR:
7.129



IMPACT FACTOR:
7.429



INTERNATIONAL JOURNAL FOR RESEARCH

IN APPLIED SCIENCE & ENGINEERING TECHNOLOGY

Call : 08813907089  (24*7 Support on Whatsapp)